Picosecond Raman Scattering

A. Laubereau

Email alerting service	Receive free email alerts when new articles cite this article - sign up in the box at the top right-hand corner of the article or click **here**

Picosecond Raman scattering

By A. Laubereau

University of Bayreuth, Bayreuth, West Germany

A survey of picosecond techniques for the study of vibrational dynamics in liquids is presented. The coherent Raman scattering of ultrashort probing pulses is discussed in more detail. A novel k-vector technique investigates the dephasing of a molecular subgroup selected from a distribution of vibrational frequencies. Experimental examples are reported which yield the (homogeneous) dephasing time and, for the first time, give direct evidence of inhomogeneous line broadening in several cases. Special emphasis is laid on the physical interpretation of the picosecond results.

In recent years, studies of vibrational dynamics in liquids have received increasing attention. Numerous investigations have been carried out with conventional infrared and Raman spectroscopy. These measurements give interesting information on a variety of physical processes which effect the molecular motion on the timescale of 10^{-12}–10^{-10} s (see Bailey 1974). The understanding of the spectroscopic data, however, is made difficult by several uncertainties. Experimental factors, e.g. measuring accuracy and finite instrumental resolution, hinder the determination of the true band contour of the vibrational transition of interest. Even more important for polyatomic molecules is the problem of overlapping neighbouring lines. Contributions by hot bands of other vibrational modes, although not properly known, have to be taken into account in many practical cases, and represent a source of experimental uncertainty. Once a band contour is determined, the question arises about its physical interpretation. In general, there are many processes that contribute to an observed band shape. Such broadening factors are rotational motion, vibrational dephasing processes, energy redistribution and transfer and an inhomogeneous distribution of vibrational transition frequencies. At the present time, one cannot isolate the different contributions by conventional spectroscopy. Additional information by other methods is highly desirable for a better understanding of the spectroscopic data.

In this article we briefly discuss new experimental techniques to study the dynamics of vibrational modes in liquids. Picosecond laser pulses are used for direct, time-resolved investigations yielding detailed information on ultrafast relaxation processes. Several recent experiments will be presented to illustrate the state of the art and the potential of our techniques.

Figure 1 schematically outlines the experimental methods. The measurements consist of two steps. First, the excitation of the molecules is achieved by an intense short laser pulse via stimulated Raman scattering or by resonant absorption of an infrared pulse. After the excitation process, free relaxation with dephasing processes and/or energy transfer of the excited mode occurs. A second, weak probe pulse properly delayed with respect to the first pulse monitors the instantaneous state of the excited vibrational system. Three probing processes are listed in figure 1, and were used to obtain different dynamical information:

(i) Coherent Raman scattering occurs from the interaction of the probe pulse with the coherently excited system. This scattering process is sensitive to the phase relation between the

[231]

442   A. LAUBEREAU

vibrating molecules and requires a carefully adjusted geometry of the relevant wave vectors (von der Linde *et al.* 1971; Laubereau 1974). It will be discussed below that time resolved coherent anti-Stokes and Stokes scattering yields direct information on vibrational dephasing processes and, for the first time, on the question of inhomogeneous line broadening in liquids (Laubereau *et al.* 1976, 1978).

(ii) Incoherent (spontaneous) anti-Stokes Raman scattering allows the study of the instantaneous occupation of a vibrational energy level. With this technique it was possible, for the first time, to measure population lifetimes, energy transfer, and energy redistribution (Laubereau *et al.* 1972; Alfano & Shapiro 1972). Time constants between 1 ps and several tens of ps were measured for different relaxation processes in a number of polyatomic molecules (Laubereau *et al.* 1973; Spanner *et al.* 1976).
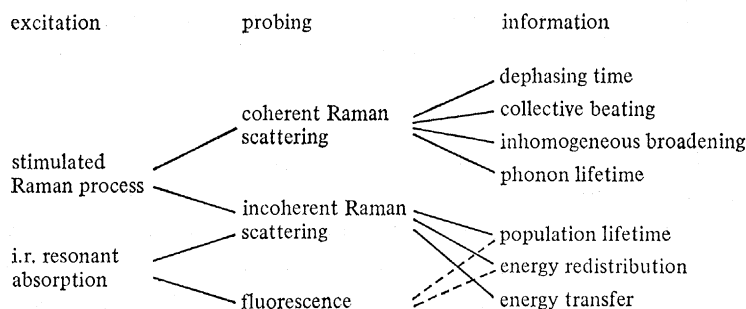

FIGURE 1. Physical processes for the excitation and the probing of molecular vibrations in liquids with picosecond light pulses. The dynamical information is listed on the right.

(iii) We have also used a fluorescence probing technique where a first infrared pulse excited a well-defined vibrational mode and a second probe pulse promoted the molecules to the fluorescent first singlet state. This technique was found very useful for investigations of highly diluted systems (Laubereau *et al.* 1975). It has been applied very recently in a novel two-pulse spectroscopy with widely tunable picosecond pulses giving new spectroscopic data on vibrational levels in the electronic ground and excited states of large polyatomic molecules (Seilmeier *et al.* 1978).

In this paper we wish to concentrate on investigations of vibrational dephasing processes with picosecond Raman techniques. The following measurements will be discussed in some detail: the dephasing time of a homogeneously broadened transition; the dephasing time of a single component of a complex vibrational system and the collective beating due to different vibrational species; and the homogeneous dephasing of a molecular subgroup selected out of an inhomogeneously broadened vibrational band by a suitable k-vector geometry.

Some theoretical remarks are given first. It is convenient to treat the vibrational system as a two-level model; transitions involving higher excited states are negligible because of the anharmonic frequency shift. In this picture the coherent interaction of a vibrational mode with a non-resonant light pulse via stimulated Raman scattering is quite analoguous to the well-known case of magnetic dipole interaction of a spin system. The stimulated scattering generates a coherent vibrational excitation represented by the amplitude $\langle q \rangle$, the expectation value of the normal mode operator. When the excitation process has terminated, $\langle q \rangle$ decays according to the dephasing time T_2: $\langle q \rangle \propto \exp(-t/T_2)$. The excess population of the excited vibrational level, on the other hand, relaxes with the population lifetime T_1 (see Laubereau & Kaiser 1977, 1978).

For the subsequent discussion it is advantageous to consider the more general case of an ensemble of two-level systems with an inhomogeneous distribution of vibrational transition frequencies. Molecules in a small frequency interval of this distribution are grouped together as vibrational components j with coherent amplitude $\langle q_j \rangle$ and with number density Nf_j, where N denotes the total number density; $(\Sigma f_j = 1)$. Introducing the absolute values Q_j and phase factors ϕ_j of the amplitudes $\langle q_j \rangle$ and also the field amplitudes E_{L} and E_{S} of the laser and Stokes scattered light, the stimulated process is described by the following set of equations (Laubereau *et al.* 1978):

$$\left(\frac{\partial}{\partial x} + \frac{1}{v_{\mathrm{S}}} \frac{\partial}{\partial t} \right) E_{\mathrm{S}} = \kappa_1 E_{\mathrm{L}} \sum_j f_j Q_j \cos\,(\Delta\omega_j t + \phi_j), \tag{1}$$

$$\left(\frac{\partial}{\partial t} + \frac{1}{T_2} \right) Q_j = \kappa_2 E_{\mathrm{L}} E_{\mathrm{S}} \cos\,(\Delta\omega_j t + \phi_j), \tag{2}$$

$$\frac{\partial}{\partial t}\,(\Delta\omega_j t + \phi_j) + \frac{\kappa_2 E_{\mathrm{L}} E_{\mathrm{S}}}{Q_j} \sin\,(\Delta\omega_j t + \phi_j) = \Delta\omega_j, \tag{3}$$

where
$$\kappa_1 = \frac{\pi\omega_{\mathrm{S}}^2 N}{c^2 k_{\mathrm{S}}} \frac{\partial\alpha}{\partial q}; \quad \kappa_2 = \frac{1}{4m(\omega_{\mathrm{L}} - \omega_{\mathrm{S}})} \frac{\partial\alpha}{\partial q}, \tag{4}$$

and
$$\Delta\omega_j = \omega_{\mathrm{L}} - \omega_{\mathrm{S}} - \omega_j. \tag{5}$$

The coupling coefficients κ_1 and κ_2 combine various material parameters (equation (4)). We assume, for all components j, equal values of the reduced molecular mass m, the Raman polarizibility $\partial\alpha/\partial q$ and the dephasing time T_2. The term v_{S} is the group velocity of the Stokes pulse. $\Delta\omega_j$ denotes the frequency distance of the molecular subgroup j from the band centre. The small population changes of the excited states which occur during the excitation process are neglected in equation (4) for the coefficient κ_1. The differential equation for the time evolution of the excited state population is not required in the subsequent discussion and is omitted here. It is readily seen that the rotational motion of the molecules does not explicitly enter equations (1)–(5). This is due to the assumption of an isotropic Raman scattering tensor, i.e. $\partial\alpha/\partial q$ is a scalar. This approximation is well justified for the experiments discussed below. A careful theoretical analysis shows that the anisotropy of the Raman scattering tensor and the molecular rotation has only negligible effect on the coherent probing technique, even for moderately large depolarization factor $\rho_{\mathrm{S}} \lesssim 0.2$. A deconvolution of rotational contributions is not required in the examples investigated below. This result is an important advantage as compared to conventional Raman spectroscopy. We have made a detailed study of equations (1)–(5) with material parameters applicable to the following experiments. Some of the findings are briefly summarized:

The excitation and subsequent free decay of the vibrational system is illustrated by numerical data depicted in figures 2–4 for three different physical situations. Figure 2 shows the simple case of a homogeneous line. The exponential decay of Q^2 with time constant $\frac{1}{2}T_2$ should be noted. In figure 3 a vibrational system with isotopic substructure is considered. The total excitation $|Q_{\mathrm{tot}}|^2 = |\Sigma f_j \langle q_j \rangle|^2$ is plotted. The free decay of the substructured system shows a beating effect which is a direct consequence of the isotopic line splitting and the approximately constant phase relation between the isotopic species established in the excitation process. The beating time reflects the constant frequency spacing $\Delta\omega$ of the vibrational components. The
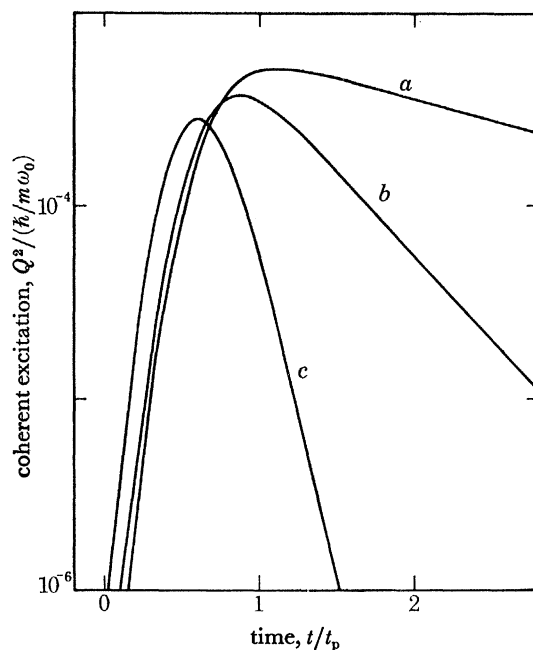
444   A. LAUBEREAU

FIGURE 2. Coherent vibrational excitation (in units of $\hbar/m\omega_0$) against time for three values of the parameter t_p/T_2 (duration of pump pulse t_p to dephasing time T_2). Note the exponential decay of the freely relaxing system with time constant $\frac{1}{2}T_2$. (a) $t_p/T_2 = 0.25$, (b) $t_p/T_2 = 1$, (c) $t_p/T_2 = 4$.
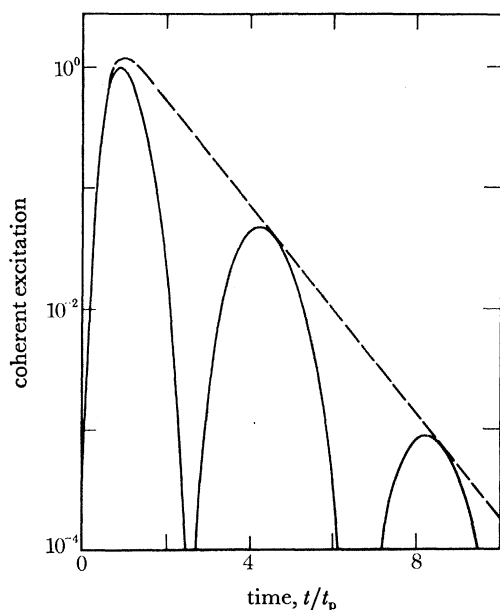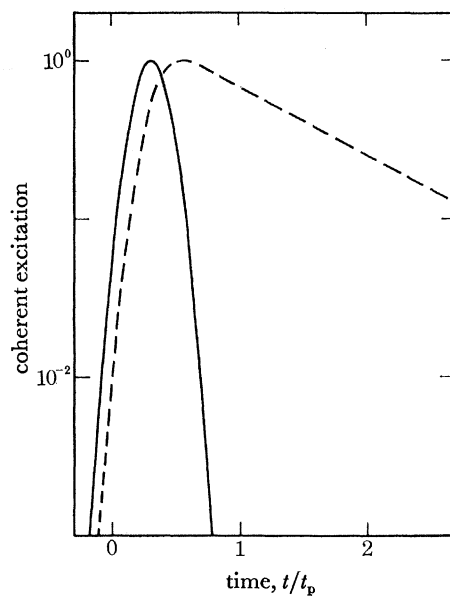

FIGURE 3

FIGURE 4

FIGURE 3. Calculated coherent vibrational excitation of three molecular components against time t/t_p assuming equal frequency spacing $\Delta\omega$ and relative abundances $1:0.5:0.5$. The solid curve represents the beating due to the superposition of the vibrational excitations. The broken line indicates the vibrational excitation of one molecular component. $t_p/T_2 = 0.5$, $\Delta\omega T_2 = \frac{1}{4}\pi$.

FIGURE 4. Calculated coherent excitation of a vibrational system with a Gaussian distribution of transition frequencies (bandwidth $\delta\omega$). The solid curve represents the total vibrational decay due to destructive interference of the various components ($|Q_{tot}|^2$). The broken line shows the time behaviour of a molecular subensemble with negligible spread of transition frequencies ($|Q_j(\Delta\omega = 0)|^2$). $t_p/T_2 = 0.5$, $T_2\delta\omega = 45$.

envelope curve decays with time constant $\frac{1}{2}T_2$. Quite different is the result shown in figure 4 for a broad (quasi-continuous) distribution of transition frequencies of width $\delta\omega_{inh} T_2 = 45$. The total coherent excitation $|Q_{tot}|^2 = |\Sigma f_j\langle q_j\rangle|^2$ disappears very rapidly in the figure on account of the broad frequency distribution. The individual components, on the other hand, decay more slowly with time constant $\frac{1}{2}T_2$.

The coherent vibrational excitation is monitored by coherent Raman scattering of a delayed probe pulse. The coherent amplitudes $\langle q_j\rangle$ give rise to a macroscopic polarization $P = N(\partial\alpha/\partial q) E \Sigma f_j\langle q_j\rangle$, where E denotes the electromagnetic field of the probe pulse. The induced polarization generates the scattering emission, which is shifted by the vibrational frequency to larger (anti-Stokes) or smaller (Stokes) frequencies.

Of particular importance is the wavevector geometry of the coherent probe scattering. The molecules vibrate with a defined spatial phase relation described by a wavevector $\boldsymbol{k}_0 = \boldsymbol{k}_L - \boldsymbol{k}_S$. The wavevector $\boldsymbol{k}_0$ is prepared during the excitation process by the laser ($\boldsymbol{k}_L$) and stimulated Stokes pulse ($\boldsymbol{k}_S$). In condensed systems, the material k-vector $\boldsymbol{k}_0$ is conserved when the excitation process terminates. The excited subgroups j behave like oscillating three-dimensional phase gratings. Scattering from these gratings occurs when the k-matching condition for the relevant wavevectors is fulfilled; i.e. the mismatch Δk_j between the incident probe pulse ($\boldsymbol{k}_{L2}$), the scattered light and the k-vector of the molecular subgroups should be sufficiently small. For Stokes scattering we have the condition:

$$|\Delta k_j|\,\Delta l = |\boldsymbol{k}_{L2} - \boldsymbol{k}_{Sj} - \boldsymbol{k}_0|\,\Delta l \lesssim 0.5. \tag{6}$$

Correspondingly, efficient anti-Stokes scattering occurs if

$$|\Delta k_j|\,\Delta l = |\boldsymbol{k}_{aj} - \boldsymbol{k}_{L2} - \boldsymbol{k}_0|\,\Delta l \lesssim 0.5. \tag{7}$$

Here, $\boldsymbol{k}_{Sj}$ and $\boldsymbol{k}_{aj}$ respectively represent the Stokes and anti-Stokes components of the probe scattering generated by the molecular subgroup j; i.e. $k_{aS,j} = (\omega_{L2} \pm \omega_j)\,n/c$. Δl is the interaction length of the probing process. It is concluded from equations (6) and (7) that only molecular subgroups with appropriate values of the transition frequency ω_j fulfil the k-matching condition. Vibrational components with mismatch $\Delta k_j\Delta l$, considerably larger than indicated by equations (6) or (7), only make negligible contributions to the probe scattering. The frequency interval of allowed transition frequencies depends on the interaction length Δl. We wish to distinguish two limiting cases (Laubereau *et al.* 1976, 1978):

(i) Selective k-matching. For large values of $\Delta l(\Delta l \gtrsim 1$ cm) a highly selective k-vector geometry may be adjusted in order to observe probe scattering of a molecular subensemble with negligible spread of transition frequencies. This subgroup is expected to decay with the (homogeneous) dephasing time.

(ii) Non-selective k-matching. For a small interaction length ($\Delta l \ll 1$ cm) the k-matching is not sensitive to the distribution of transition frequencies and coherent superposition of the various molecular components may be observed. In this case interesting beating effects or dephasing of the molecules by the distribution of transition frequencies was investigated; i.e. the total coherent excitation discussed above in context with figures 3 and 4 can be studied. The different values of Δl are experimentally adjusted by varying the scattering geometry (e.g. sample length).

Our experimental system for time-resolved coherent Raman scattering with collinear wavevector geometry is depicted schematically in figure 5. For the generation of the ultra-short light pulses we use a Nd/glass laser system consisting of a mode-locked laser oscillator, an

electro-optic switch to select a single pulse, and a laser amplifier. We emphasize the need to work with single bandwidth limited pulses of well defined duration, pulse shape, frequency width, and peak intensity. Bandwidth limited pulses are required in our investigations to achieve high k-vector resolution. After frequency doubling in a KDP crystal we work with pulses of frequency $\nu_L = 18910$ cm^{-1}, width $\delta\nu_L \approx 5$ cm^{-1}, pulse duration $t_p \approx 3.5$ ps and approximately Gaussian shape. Stimulated Raman scattering is effectively generated in samples of several centimetres of length. A beam splitter in the path of the incident pulse provides a second pulse of small intensity (approximately 10^{-2} of the exciting pulse). The weak pulse serves as a probing pulse; it passes a variable delay device and a second beam splitter,
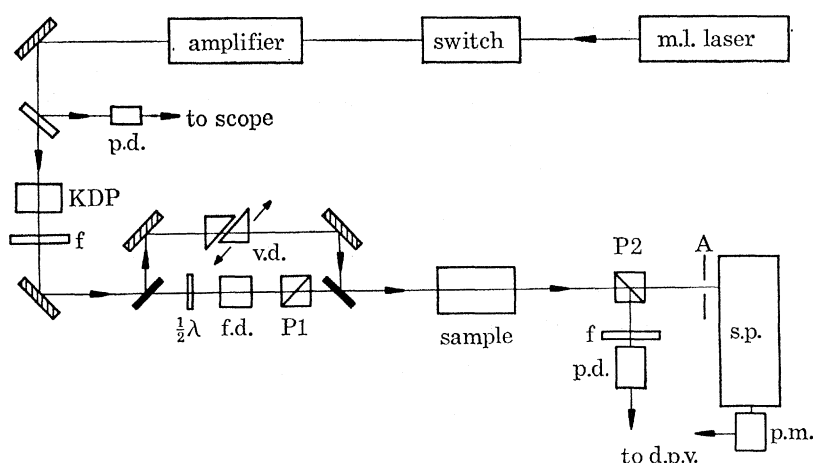

FIGURE 5. Experimental arrangement for measuring coherent Raman probe scattering of picosecond pulses in a collinear geometry. A beam splitter generates the probe pulse which is properly delayed before travelling collinearly with the exciting pulse. The scattered signals of the two pulses are separated by two polarizers P1 and P2; fixed delay f.d., variable delay v.d., filter f, photodetectors p.d. and p.m., spectrometer sp, digital peak voltmeter d.p.v.

so that the probe pulse travels parallel to the excitation pulse. In a number of experiments, non-collinear systems (not shown here) have been also used. Owing to the k-matching requirements, the coherent Raman scattering signal is highly collimated and observed in the forward direction as a function of time delay between excitation and probing pulse. In figure 5 the scattering emissions of the excitation and probing processes are distinguished using perpendicular planes of polarization. The pump pulse passes a $\frac{1}{2}\lambda$ plate and polarizer P1 defining the plane of polarization of the excitation process. The stimulated scattering of the pump pulse is effectively blocked by a factor of ca. 10^5 with the help of the second polarizer P2. The probe pulse and the corresponding coherent scattering signal, on the other hand, pass P2 without significant attenuation. An aperture, A, determines the angle of acceptance of the detection system consisting of a spectrometer and a photo-multiplier.

Observing coherent probe scattering at the Stokes side of the spectrum with the collinear geometry of figure 5 gives optimum k-vector resolution. By using long samples (length 10 cm) and taking into account additional factors, such as the finite divergence of the light beams, we expect a high k-resolution of our picosecond experiment corresponding to a frequency resolution $\delta\tilde{\nu}$ of a few tenths of a wavenumber (cm^{-1}).

As an example of homogeneous line broadening we discuss the symmetrical CH$_3$-stretching mode of CH$_3$CCl$_3$ at 2939 cm^{-1}. Figure 6 presents the picosecond data on the dephasing time

of the molecular vibration. The coherent probe scattering signal is plotted as a function of delay time between excitation and probe pulse. From the exponential decay of the signal curve we deduce a dephasing time of $\frac{1}{2}T_2 = 1.2$ ps, which corresponds to a homogeneous line broadening of 4.3 cm^{-1}. This number is an excellent agreement with the linewidth of the isotropic scattering component observed in spontaneous Raman spectroscopy; i.e. the dynamic processes described by the dephasing time T_2 (pure dephasing and population relaxation) fully account for the spectroscopic line broadening. We have also investigated the population lifetime T_1 of the first excited level of the same vibrational mode (Laubereau et al. 1972, 1973). A value of $T_1 = 5.2$ ps was found for the pure liquid. The difference between the time constants $\frac{1}{2}T_2$ and T_1 indicates that the phase correlation between the CH_3CCl_3 molecules may be lost under conservation of the excited state population (pure dephasing). Investigations of the coherent probe scattering under different geometries give no indication of an inhomogeneous broadening of this mode within experimental accuracy; i.e. the measurements set an upper limit of $\delta\tilde{\nu}_{inh} \lesssim 0.6$ cm^{-1} for a possible small inhomogeneous line broadening.
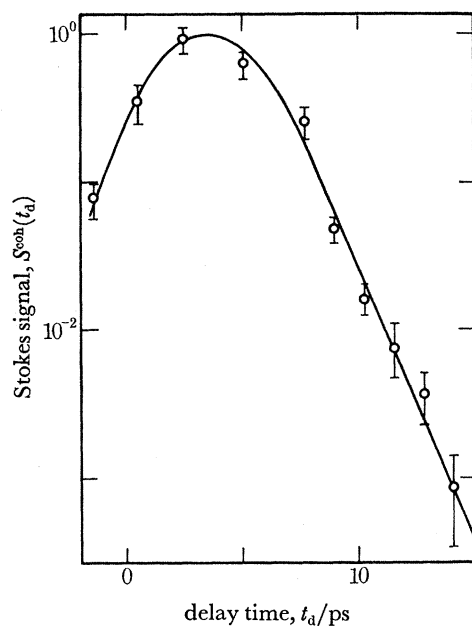

FIGURE 6. Coherent probe scattering signal $S^{coh}(t_d)$ against delay time between pump and probe pulse for the symmetric CH_3 stretching mode of CH_3CCl_3 (295 K). $\tilde{\nu} = 2939$ cm^{-1}, $\frac{1}{2}T_2 = 1.2 \pm 0.2$ ps.

A more complex situation is found for molecular vibrations with isotopic substructure. For these cases the observed time dependence of the coherent probe scattering depends on the k-matching situation. CCl_4 is discussed here as an example. The two isotopes ^{35}Cl and ^{37}Cl give rise to vibrational multiplicity of the totally symmetric tetrahedral vibration around 460 cm^{-1}. The isotopic structure is clearly seen in the spontaneous Raman spectrum with a frequency spacing of approximately 3 cm^{-1} of the various lines (see inset of figure 7(a)). The results for coherent probe scattering with a selective k-geometry are depicted in figure 7(a) (Laubereau et al. 1976). The decaying part of the signal curve represents loss of phase correlation of a single isotopic component with time constants $\frac{1}{2}T_2 = 3.6$ ps. The measured dephasing time fully accounts for the Raman linewidth for one isotopic species of 1.4 cm^{-1}. Additional

information is obtained by coherent probing with non-selective k-matching. In these experiments, a coherent superposition of the different isotopic species is observed (figure 7(b)). The various isotopic components are first excited with approximately equal phases (rising part of the signal curves). The excitation process then terminates, and free relaxation of the collective excitation is observed. The frequency differences of the individual species lead to a striking interference phenomenon with a beating period of *ca*. 12 ps, in good agreement with the theoretical results of figure 3.
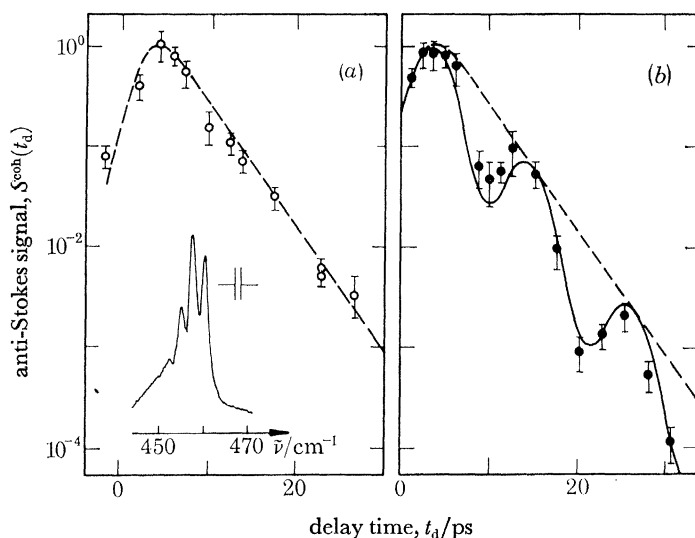

FIGURE 7. Coherent probe scattering $S^{coh}(t_d)$ against delay time for CCl_4 with natural isotopic abundance; (*a*) selective k-matching observing a single isotope component; (*b*) non-selective k-matching with coherent superposition of vibrational states; curves are calculated. Inset: spontaneous Raman band. $\frac{1}{2}T_2 = 3.6 \pm 0.4$ ps.

There are vibrational modes where experimental evidence exists of a distribution of transition frequencies. For instance, liquids with strong hydrogen bonding show extended OH-bands, which are believed to be inhomogeneously broadened. Spontaneous spectroscopic techniques provide the total Raman or infrared band, but do not allow a separation between homogeneous and inhomogeneous broadening factors. As a result it is impossible, in general, to decide to what extent a band contour contains inhomogeneous contributions. Our coherent Raman probing technique allows us to study this problem for the first time. The vibrational system which is investigated here is the CH-stretching mode of pure $(CH_2OH)_2$ at 2935 cm^{-1}. The spontaneous Raman band of this mode is broad with a linewidth of *ca*. 60 cm^{-1} (see figure 9). In figure 8 we present experimental data of two widely different experimental situations (Laubereau *et al.* 1978). In figure 8(a), a highly selective k-matching situation is used with a sample length of 10 cm and with a small divergence of the Stokes beam of 3 mrad. In figure 8(b), on the other hand, we devised a less selective k-vector geometry by using a shorter cell of 1 cm and a larger Stokes divergence of 10 mrad. Comparison of the two geometries gives information on the question of inhomogeneous broadening.

The experimental results of figure 8(a) are of special interest. After the maximum of the probe signal we find an exponential decay with a time constant of $\frac{1}{2}T_2 = 3.0 \pm 0.5$ ps. For an interpretation of this time constant we estimate the frequency spread of the molecules monitored by the selective k-vector geometry to be smaller than 0.5 cm^{-1}; i.e. dephasing by a

distribution of frequencies is negligible. The time constant of 3 ps represents the homogeneous dephasing of a small group of molecules, the frequency of which is close to the centre frequency of the broad Raman band at 2935 cm^{-1}.

The time dependence of $S^{coh}(t_d)$ is completely different for less selective phase matching (figure 8b). Under these experimental conditions the coherent scattering signal disappears rapidly. The measured time dependence represents the destructive interference of molecules which vibrate with a wide distribution of frequencies. The picosecond data of figure 8 provide direct evidence that the vibrational band is inhomogeneously broadened.
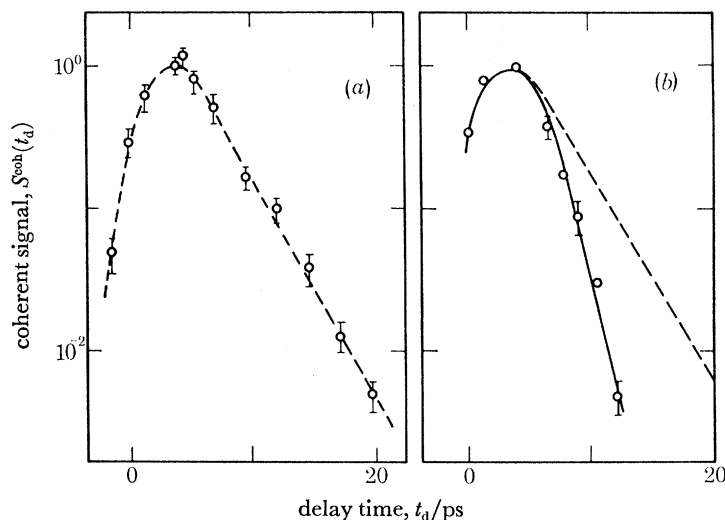

FIGURE 8. (a) Coherent Stokes scattered probe signal $S^{coh}(t_d)$ against delay time measured in a highly selective collinear k-matching geometry in $(CH_2OH)_2$. We observe a dephasing time $\frac{1}{2}T_2 = 3.0$ ps of the C—H mode at 2935 cm^{-1}, corresponding to a homogeneous linewidth of 1.8 cm^{-1}. (b) Coherent Stokes signal $S^{coh}(t_d)$ for a less selective k-matching geometry. The signal decays rapidly on account of destructive interference of neighbouring molecules oscillating with different transition frequencies. Comparison of (a) and (b) gives direct evidence of inhomogeneous line broadening.

It is interesting to compare these results with spontaneous Raman data. Our value of T_2 corresponds to a Lorentzian of width 1.8 cm^{-1} which is indicated in the Raman spectrum of figure 9. It is readily seen that the homogeneous line is smaller than the total band by a factor of approximately 30. Similar results were obtained for the C—H mode of pure CH_3OH at 2835 cm^{-1} and are also indicated in figure 9. For this mode, dephasing of a molecular sub-group was observed corresponding to a Lorentzian of 2.3 cm^{-1}. This homogeneous broadening is considerably smaller than the total (inhomogeneous) Raman band.

Our findings of figures 8 and 9 point to at least two different mechanisms which proceed on vastly different time scales and determine the dynamics of the investigated C—H modes. The first mechanism leading to the observed exponential decay with time constants T_2 of several picoseconds is obviously close to the limit of motional narrowing, i.e. this mechanism occurs on a rapid timescale < 1 ps. The second mechanism is responsible for the inhomogeneous broadening. This interaction has to proceed on a comparatively long time scale (> 10^{-11} s), much longer than the duration of our picosecond experiment, in order to allow us the observation of a distribution of transition frequencies. Owing to motional narrowing, the rapid interaction produces quite narrow homogeneous lines, while the slow mechanism generates broad band shapes of several 10 cm^{-1} in the case of the investigated alcohols.

[239]

While significant inhomogeneous broadening is not surprising for broad Raman bands of systems with strong hydrogen bonding, the question arises about the situation in weakly associated liquids. As an example we briefly summarize very recent results on deuterated benzene C_6D_6 (Laubereau *et al.* 1979). The totally symmetric ring vibration at 945 cm^{-1} gives rise to an intense and very narrow Raman line of width 1.5 cm^{-1}. We have investigated this mode with our picosecond Raman technique and found very interesting results. With the
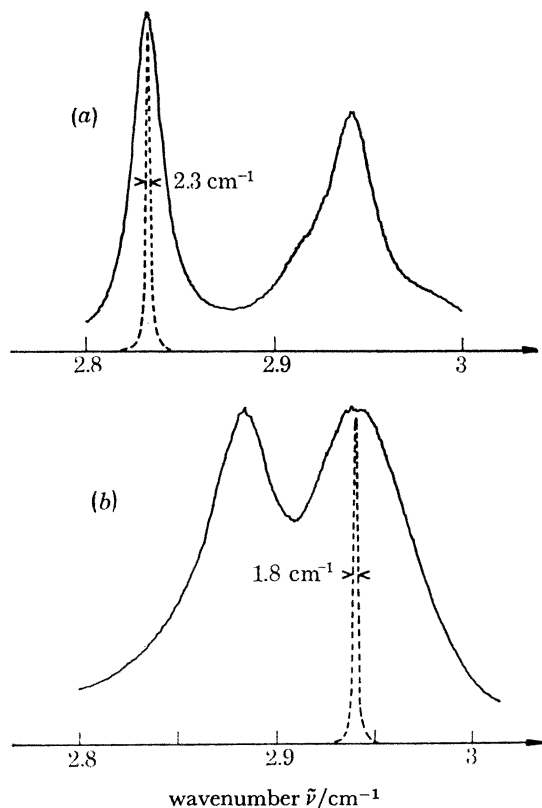

FIGURE 9. Spontaneous Raman spectrum (polarized scattering component) of the CH modes in (a) CH$_3$OH and (b) (CH$_2$OH)$_2$ at 2835 and 2935 cm^{-1}, respectively, which were investigated by coherent Raman probe scattering. The homogeneous line broadening of the observed molecular subgroups at the centre of the Raman bands is indicated.

experimental apparatus of figure 5, we have measured the coherent probe scattering under a selective k-vector geometry. Monitoring the signal decay over a factor of 200 we observe approximately exponential relaxation with a time constant of $\frac{1}{2}T_2 = 5.0 \pm 0.5$ ps. For non-selective k-matching conditions, on the other hand, we measure a notably accelerated signal decay indicating additional dephasing by a distribution of vibrational frequencies. For an assumed Gaussian frequency distribution, a theoretical curve was fitted to the picosecond data in order to determine the linewidth of the inhomogeneous broadening. We find a value of $\delta\tilde{\nu}_{\mathrm{inh}} = 0.6 \pm 0.2$ cm^{-1}. Additional support to our picosecond results is obtained by a comparison with the spontaneous Raman band. The value of $T_2 = 10$ ps corresponds to a homogeneous broadening of Lorentzian shape and width $\delta\tilde{\nu}_{\mathrm{hom}} \approx 1.0$ cm^{-1}. Convolution of the homogeneous and inhomogeneous contribution leads to a Voigt profile which agrees well with our measured band contour of the polarized scattering component of this mode.

To summarize the picosecond investigations, the following preliminary physical picture is proposed:

(i) We emphasize the clear evidence for a distribution of vibrational frequencies in several strongly and weakly associated liquids. The important point here is the timescale on which the vibrational frequency of molecules may fluctuate. Our data suggest the frequency distribution to be static for at least 10^{-11} s or even longer. The different frequencies of the individual molecules result from variations of the solvent shift exerted by the molecular environment. Existing static theories successfully explain the well-known frequency shifts of the band centres in liquid systems (Buckingham 1958). More elaborate stochastic theories also reveal the relationship with the frequency distribution (Bratos *et al.* 1970). In the limiting case of inhomogeneous broadening one may write for the frequency shift, $\Delta\omega$,

$$\Delta\omega = Z\delta, \tag{8}$$

where Z is the effective number of interacting molecules and δ denotes the frequency shift generated by one neighbouring molecule. Variations of the number of interacting neighbours generates a finite frequency width $\delta\omega_{\text{inh}}$:

$$\delta\omega_{\text{inh}} = Z^{\frac{1}{2}}\delta. \tag{9}$$

Combining the two equations gives the simple relation

$$\delta\omega_{\text{inh}} = \Delta\omega/Z^{\frac{1}{2}}. \tag{10}$$

Although there are additional processes affecting the vibrational dynamics, it appears that these interactions generate only negligible frequency shifts (limit of motional narrowing, see below). For this reason experimental numbers of the solvent shift may be used for $\Delta\omega$ in equation (10). For weakly associated liquids, $\Delta\omega$ has the order of magnitude of several cm^{-1}, so that somewhat smaller values are suggested for $\delta\omega_{\text{inh}}$ by equation (10). All details of the intermolecular interaction are contained in the number Z which may be evaluated by a microscopic theory. For benzene our value of $\delta\omega_{\text{inh}} = 0.6$ cm^{-1} and the reported frequency shift of $\Delta\omega = 4$ cm^{-1} (Nestor & Lippincott 1973) yields $Z \approx 50$; i.e. a large number of molecules determine the frequency position of an individual molecule, suggesting interaction via the long-range (attractive) part of the intermolecular potential. This conclusion is consistent with the slow timescale of the interaction required for inhomogeneous broadening. Molecules enter or leave the comparatively large interaction volume by diffusional motion, which proceeds on the time scale of *ca.* 10^{-10} s.

(ii) There is additional evidence for rapid relaxation processes. These processes are collected by the (homogeneous) dephasing time T_2. An important point is the timescale of these interactions. In order to explain the exponential decay observed over several orders of magnitude for a number of examples the limiting case of homogeneous broadening with motional narrowing must be considered. In other words, a time scale of *ca.* 1 ps or less is required for the individual interaction event. It is suggested that the small amplitude rattling motion of the molecules in their liquid cages is a major factor for these processes, which occurs on the timescale of *ca.* 10^{-13} s. Coupling to rotational motion which is also fast ($\lesssim$ 1 ps) in general may also be important. The following processes have been suggested to contribute to the measured T_2 values of polyatomic molecules:

(*a*) 'direct' dephasing by quasi-elastic nearest neighbour interaction via the repulsive part of

the intermolecular potential (Fischer & Laubereau 1975; Madden & Lynden-Bell, 1976; Rothschild 1976; Wertheimer 1978);

(b) indirect dephasing by anharmonic coupling to low frequency vibrational modes (Bratos 1975; Fischer & Laubereau 1978);

(c) resonant exchange of vibrational quanta via the repulsive part of the intermolecular potential or transition dipole–dipole interaction (Döge et al. 1977; Gilbert & Drifford 1977);

(d) energy transfer to neighbouring vibrational levels converting small energy mismatches to rotational and translational motion (Miklavc & Fischer 1976).

Processes (d) can be distinguished from the mechanisms (a)–(c) that measure the time evolution of the excited state population (T_1-techniques), not discussed in the present paper. Some information on vibrational–translational transfer is also gained from ultrasonic and hypersonic dispersion or absorption studies.

For our example CH_3CCl_3 (figure 6) theoretical estimates suggest process (a) as the dominant T_2 mechanism while process (b) appears to be unimportant (Fischer & Laubereau 1978). The small concentration dependence of the linewidth also rules out a significant contribution of (c). Approximately 20 % of the total line broadening is due to population decay (d). For the other modes investigated above, the dominant mechanism of T_2 cannot be stated definitely at the present time.

In conclusion, it is pointed out that several new techniques have been developed for the investigation of vibrational dynamics in liquids. These experiments benefit from the specific non-equilibrium situations of the vibrational system established with well-understood excitation processes and the high time resolution available with picosecond light pulses. For the coherent Raman probing technique, the generated phase relation of molecules contained in a macroscopic excitation volume has been shown to be an important factor. It offers the possibility of selecting a molecular subgroup by k-vector spectroscopy and gives new and detailed information on relaxation phenomena. Further application of the picosecond techniques will give deeper insight in the liquid state and will advance our understanding of the ultrafast molecular dynamics.

REFERENCES (Laubereau)

Alfano, R. R. & Shapiro, S. L. 1972 *Phys. Rev. Lett.* **29**, 1655–1659.
Bailey, R. T. 1974 In *Molecular spectroscopy*, vol. 2. London: The Chemical Society.
Bratos, S. 1975 *J. chem. Phys.* **63**, 3499.
Bratos, S., Rios, J. & Guissany, Y. 1970 *J. chem. Phys.* **52**, 439–452.
Buckingham, A. D. 1958 *Proc. R. Soc. Lond.* A **248**, 169–182.
Döge, D., Arndt, R. & Khuen, A. 1977 *Chem. Phys.* **21**, 53–59.
Fischer, S. F. & Laubereau, A. 1975 *Chem. Phys. Lett.* **35**, 6–12.
Fischer, S. F. & Laubereau, A. 1978 *Chem. Phys. Lett.* **55**, 189–196.
Gilbert, M. & Drifford, M. 1977 *J. chem. Phys.* **66**, 3205–3214.
Laubereau, A. 1974 *Chem. Phys. Lett.* **27**, 600–602.
Laubereau, A. & Kaiser, W. 1977 In *Chemical and biochemical applications of lasers* (ed. C. B. Moore), vol. 2. New York: Academic Press.
Laubereau, A. & Kaiser, W. 1978 *Rev. mod. Phys.* (to be published).
Laubereau, A., Kirschner, L. & Kaiser, W. 1973 *Opt. Commun.* **9**, 182–185.
Laubereau, A., Seilmeier, A. & Kaiser, W. 1975 *Chem. Phys. Lett.* **36**, 232–237.

Laubereau, A., von der Linde, D. & Kaiser, W. 1972 *Phys. Rev. Lett.* **28**, 1162–1165.
Laubereau, A., Wochner, G. & Kaiser, W. 1976 *Phys. Rev.* A **13**, 2212–2225.
Laubereau, A., Wochner, G. & Kaiser, W. 1978 *Chem. Phys.* **28**, 363–369.
Laubereau, A., Wochner, G. & Kaiser, W. 1979 (to be published).
Madden, P. A. & Lynden-Bell, R. M. 1976 *Chem. Phys. Lett.* **38**, 163.
Miklavc, A. & Fischer, S. F. 1976 *Chem. Phys. Lett.* **44**, 209–213.
Nestor, J. R. & Lippincott, E. R. 1973 *J. Raman Spectrosc.* **1**, 305–318.
Rothschild, W. G. 1976 *J. chem. Phys.* **65**, 2958.
Seilmeier, A., Kaiser, W. & Laubereau, A. 1978 *Opt. Commun.* (to be published).
Spanner, K., Laubereau, A. & Kaiser, W. 1976 *Chem. Phys. Lett.* **44**, 88–92.
von der Linde, D., Laubereau, A. & Kaiser, W. 1971 *Phys. Rev. Lett.* **26**, 954–957.
Wertheimer, R. K. 1978 *Molec. Phys.* **35**, 257–282.